Numerical analysis of superconducting phases in the extended Hubbard model with non-local pairing

University of Pisa, a.y. 2025-2026

Alessandro Gori*

Thesis for the Master's degree in Physics

Abstract

[To be continued...]

Contents

*a.gori23@studenti.unipi.it / nepero27178@github.com

List of symbols and abbreviations

AF	Anti-Ferromagnetic
BCS	Bardeen-Cooper-Schrieffer (theory)
DoF	Degree of Freedom
HF	Hartree-Fock
MFT	Mean-Field Theory
SC	Superconductor
T_c	Critical temperature

Chapter 1

Theoretical introduction

[To be continued...]

1.1 Antiferromagnetic ordering in the Hubbard model

Consider the ordinary Hubbard model:

$$\hat{H} = -t \sum_{\langle ij \rangle} \sum_{\sigma} \hat{c}^{\dagger}_{i\sigma} \hat{c}_{j\sigma} + U \sum_{i} \hat{n}_{i\uparrow} \hat{n}_{i\downarrow} \qquad t, U > 0 \tag{1.1}$$

The two competing mechanisms are site-hopping of amplitude t and local repulsion of amplitude U. For this model defined on a bipartite lattice at half filling and fixed electron number, it is well known [6] that, below a certain critical temperature T_c and above some (small) critical repulsion U_c/t, the ground-state acquires antiferromagnetic (AF) long-range ordering. schematically depicted in Fig. 1.1a. The mechanism for the formation of the AF phase takes advantage of virtual hopping, as described in App. **??**; the Mean-Field Theory (MFT) treatment of ferromagnetic-antiferromagnetic orderings in 2D Hubbard lattices is discussed in App. **??**.

In this chapter the discussion is limited to the two-dimensional square lattice Hubbard model. The lattice considered has L_ℓ sites on side $\ell = x, y$, thus a total of $L_x L_y$ sites. The total number of single electron states is given by $D = 2L_x L_y$. All theoretical discussion neglects border effects, thus considering $D \to +\infty$.

1.2 The Extended Fermi-Hubbard model

The Extended Fermi-Hubbard model is defined by:

$$\hat{H} = -t \sum_{\langle ij \rangle} \sum_{\sigma} \hat{c}^{\dagger}_{i\sigma} \hat{c}_{j\sigma} + U \sum_{i} \hat{n}_{i\uparrow} \hat{n}_{i\downarrow} - V \sum_{\langle ij \rangle} \sum_{\sigma\sigma'} \hat{n}_{i\sigma} \hat{n}_{j\sigma'} \tag{1.2}$$

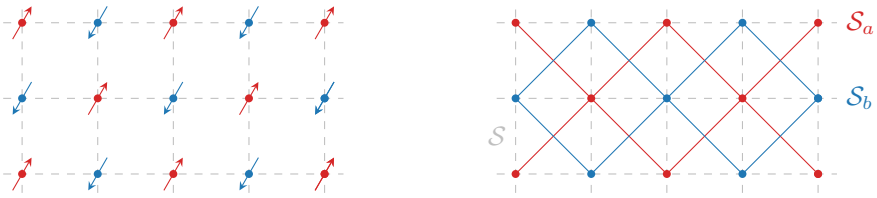

a | Antiferromagnetic phase. b | Polarized sublattices.

Figure 1.1 | Schematic representation of the AF phase. Fig. 1.1a shows a portion of the square lattice with explicit representation of the spin for each site. Fig. 1.1b divides the square lattice $\mathcal{S}$ in two polarized sublattices $\mathcal{S}_a$, $\mathcal{S}_b$. The AF phase results from the interaction of two inversely polarized "ferromagnetic" square lattices.

Note that, on a square lattice, we can perform the summation over NN just as

$$\sum_{\langle ij \rangle} \equiv \sum_{i \in \mathcal{S}_a} \left[\delta_{j=i+\delta_x} + \delta_{j=i-\delta_x} + \delta_{j=i+\delta_y} + \delta_{j=i-\delta_y} \right]$$

where notation of Fig. 1.1b has been used. The last term represents an effective attraction between neighboring electrons, of amplitude V. Such an interaction is believed [1] necessary to describe the insurgence of high-T_c superconductivity in cuprate SCs. [To be continued...]

1.2.1 Experimental insight on NN attraction

[Add:

- High T_c SC in cuprates;
- Experimental evidence of topological SC;
- Insertion of the non-local attraction;

]

Part I

Mean-Field-Theory analysis

Chapter 2

Mean-field theory discussion of the EHM

This chapter is devoted to develop a Mean Field Theory (MFT) framework of the Extended Hubbard model (EHM) of Eq. (1.2),

$$\hat{H} = \underbrace{-t \sum_{\langle ij \rangle} \sum_{\sigma} \hat{c}^{\dagger}_{i\sigma} \hat{c}_{j\sigma}}_{\hat{H}_t} \underbrace{+U \sum_{i} \hat{n}_{i\uparrow} \hat{n}_{i\downarrow}}_{\hat{H}_U} \underbrace{-V \sum_{\langle ij \rangle} \sum_{\sigma\sigma'} \hat{n}_{i\sigma} \hat{n}_{j\sigma'}}_{\hat{H}_V}$$

Mean Field Theory (MFT) is a widely used and simple theoretical tool, often sufficient to describe the leading orders in phase transition phenomena of Many-Body Physics. Here MFT is employed generically, in order to later discuss both the effects of the non-local term $\hat{H}_V$ onto the AF phase (Chap. **??**), as well as the insurgence of anisotropic superconductivity (Chap. 3). The latter, following the path of Bardeen-Cooper-Schrieffer (BCS) theory in describing conventional s-wave superconductivity. As will be thoroughly described, the lattice spatial structure directly influences the topology of the gap function, giving rise to anisotropic pairing.

[Move this part to Chap. 3] Sec. **??** studies the non-local attraction $\hat{H}_V$ in real-space, describing how such interaction can contribute to the hamiltonian as a symmetry-breaking term in given channels. In the following sections, we move to specific channels and study theoretically and numerically the effect of non-local attraction.

2.1 Extended Hubbard model symmetries and Wick's theorem

The general aim is to study the phase diagram of the model by comparing ground-state energies of different phases. The phases we consider in next chapters for the EHM are the Anti-Ferromagnetic ordering (AF), given by a non-uniform distribution of charge in each spin sector, and the Superconducting phase, described by a uniformly distributed charge allowing for Cooper pairing instabilities. For the EHM, three symmetries are "brekable":

1. Discrete translational invariance. By breaking explicitly this symmetry, the obtained state must show a Charge-Density Wave (CDW) ordering;

2. $\mathrm{U}^{\mathrm{c}}(1)$ charge conservation. By breaking this symmetry, we allow for the total charge to fluctuate in the ground state;

3. SU(2) spin rotation symmetry. If this symmetry is broken, we allow for the ground state to exhibit a preferred spin direction.

4. Note that the SU(2) group contains a U(1) subgroup. SU(2) symmetry can be broken, selecting a particular vectorial direction for the order parameter, and reduced to a smaller $\mathrm{U}^{z}(1)$ symmetry which is essentially expressed by the conservation of the *magnitude* of the order parameter. [Add graphics of SU(2) $\rightarrow$ $\mathrm{U}^{z}(1)$ symmetry breaking.]

The last point is important: for the AF phase, for example, there is no need for the magnetization vector to be directed along the *real* z-axis, which is the one perpendicular to the lattice plane. SU(2)

Symmetry group	Operations
Point group	Discrete translations on lattice
$\mathrm{U^c}(1)$	Charge-conserving global phase shifts
SU(2)	Three-dimensional rotations in spin space
$\mathrm{U}^z(1)$	Reduced two-dimensional rotations around Néel z-axis in spin space

Table 2.1 | Model symmetries and relative group operations. Note that $U^{\mathrm{c}}(1)$ represents the charge conserving group, while $\mathrm{U}^z(1)$ represents the subgroup obtained by breaking the SU(2) symmetry with a vector order parameter and preserving its amplitude.

symmetry breaks when (staggered) magnetization is established along a particular direction, but spin rotations around said direction still are ground state symmetries. The symmetries are reported synthetically in Tab. 2.1.

Different phases are described by different order parameters, each one exhibiting a specific symmetry subset from the initial set, while the rest are broken. Ferromagnetic state perform $\mathrm{SU}(2) \to \mathrm{U}^z(1)$ symmetry breaking, Anti-Ferromagnetic breaks also translational invariance (reducing it to a smaller symmetry, relative to double-sized unitary cells). Basic superconducting models do not break translational invariance and can preserve full SU(2) symmetry, while breaking $\mathrm{U^c}(1)$ charge conservation. The three phases hereby considered do not completely break translational invariance: the latter either is left untouched or is reduced to a weaker translational invariance. Because of this, it will be rather useful to move the framework to reciprocal space. We will get there in Sec. **??**.

App. **??** describes in detail the MFT treatment of the pure Hubbard model, $\hat{H}_t + \hat{H}_U$ and its AF phase; the key passage is there given by the approximation

$$\hat{n}_{i\uparrow}\hat{n}_{i\downarrow} \simeq \hat{n}_{i\uparrow}\langle\hat{n}_{i\downarrow}\rangle + \langle\hat{n}_{i\uparrow}\rangle\hat{n}_{i\downarrow} + (\text{constants}) \tag{2.1}$$

from which the AF structure is simply recovered. However, to perform the above approximation coherently, we are implementing Wick's Theorem on the generic term:

$$\langle\hat{c}^\dagger_{i\sigma}\hat{c}^\dagger_{j\sigma'}\hat{c}_{j\sigma'}\hat{c}_{i\sigma}\rangle \simeq \underbrace{\langle\hat{c}^\dagger_{i\sigma}\hat{c}^\dagger_{j\sigma'}\rangle\langle\hat{c}_{j\sigma'}\hat{c}_{i\sigma}\rangle}_{\text{Cooper}} - \underbrace{\langle\hat{c}^\dagger_{i\sigma}\hat{c}_{j\sigma'}\rangle\langle\hat{c}^\dagger_{j\sigma'}\hat{c}_{i\sigma}\rangle}_{\text{Fock}} + \underbrace{\langle\hat{c}^\dagger_{i\sigma}\hat{c}_{i\sigma}\rangle\langle\hat{c}^\dagger_{j\sigma'}\hat{c}_{j\sigma'}\rangle}_{\text{Hartree}} \tag{2.2}$$

As a first approximation, the theorem is assumed to hold (which, in a BCS-like fashion, is equivalent to assuming for the ground-state to be a coherent state). The AF ground state breaks translational invariance and reduces rotational symmetry, $\mathrm{SU}(2) \to \mathrm{U}^z(1)$. Thus, of the three terms above, when considering the pure Hubbard model:

- Cooper fluctuations are suppressed, because they break charge conservation;
- Similarly the Fock term is null as well because if $i = j$ and $\sigma' = \overline{\sigma}$ (as is for the local interaction, which contains the operator $\hat{n}_{i\uparrow}\hat{n}_{i\downarrow}$) the expectation values involved are describing a process breaking the survivor $\mathrm{U}^z(1)$ spin symmetry.

Thus, correctly, the Wick's decomposition of Eq. (2.1) only involves Hartree-terms of Eq. (2.2). In general, however, the three terms need to be considered altogether: this is what is done in the next chapters.

2.1.1 Particle-hole symmetry

[To be continued...]For now, let us focus on the non-local term showing how can it break symmetries.

2.2 The non-local term as a source of symmetry-breaking interactions

Consider now the NN non-local term,

$$\hat{H}_V \equiv -V \sum_{\langle ij\rangle} \sum_{\sigma\sigma'} \hat{n}_{i\sigma}\hat{n}_{j\sigma'} \tag{2.3}$$

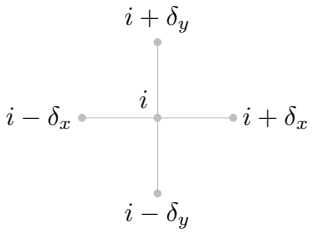

Figure 2.1 | Schematic representation of the four NNs of a given site i for a planar square lattice.

Evidently the hamiltonian can be decomposed in various spin terms,

$$\begin{aligned}\hat{H}_V &= \sum_{\sigma\sigma'} \hat{H}_V^{\sigma\sigma'} \\ &= \underbrace{\hat{H}_V^{\uparrow\uparrow} + \hat{H}_V^{\downarrow\downarrow}}_{\text{Same-spin}} + \underbrace{\hat{H}_V^{\uparrow\downarrow} + \hat{H}_V^{\downarrow\uparrow}}_{\text{Opposite-spin}}\end{aligned} \tag{2.4}$$

The role of said terms is crucial in establishing the pairing channel of the dominating physical phase. As an example, the s.s. terms can be seen as a possible source of triplet pairing superconductivity. Next section are devoted to analyze said terms and derive a simple analytical result in reciprocal space.

2.2.1 Real space description

Let us start from the real space form of Eq. (2.4). To carry out a summation over nearest neighbors $\langle ij\rangle$ of a square lattice means precisely to sum over all links of the lattice. Then we can identify the generic opposite-spin (o.s.) term $\hat{H}_V^{\sigma\overline{\sigma}}$ as the one collecting the σ operators of sublattice $\mathcal{S}_a$ and $\overline{\sigma}$ operators of sublattice $\mathcal{S}_b$. The o.s. non-local interactions can be written as a sum of terms over just one of the two sublattices $\mathcal{S}_a$ and $\mathcal{S}_b$, oppositely polarized in the AF configuration (see Fig. 1.1b)

$$\begin{aligned}\hat{H}_V^{(\text{o.s.})} &= \overbrace{\sum_{i\in\mathcal{S}_a} \hat{h}_V^{(i)}}^{\hat{H}_V^{\uparrow\downarrow}} + \overbrace{\sum_{i\in\mathcal{S}_b} \hat{h}_V^{(i)}}^{\hat{H}_V^{\downarrow\uparrow}} \\ &= \sum_{i\in\mathcal{S}} \hat{h}_V^{(i)}\end{aligned} \qquad \hat{h}_V^{(i)} = -V \sum_{\ell=x,y} (\hat{n}_{i\uparrow}\hat{n}_{i+\delta_\ell\downarrow} + \hat{n}_{i\uparrow}\hat{n}_{i-\delta_\ell\downarrow})$$

Here the notation of Fig. 1.1b is used. The two-dimensional lattice is regular-square. For each site i in a given sublattice, the nearest neighbors sites are four – all in the other sublattice. The notation used is $i\pm\delta_x$, $i\pm\delta_y$ as in Fig. 2.1. Similarly, the same-spin (s.s.) hamiltonian decomposes as

$$\hat{H}_V^{(\text{s.s.})} = -V \sum_{i\in\mathcal{S}_a} \sum_{\ell=x,y} \sum_{\sigma} (\hat{n}_{i\sigma}\hat{n}_{i+\delta_\ell\sigma} + \hat{n}_{i\sigma}\hat{n}_{i-\delta_\ell\sigma})$$

Note here the summation only on one sublattice. The non-local interaction contribution to energy, as a function of the $T=0$ full hamiltonian ground-state[1] $|\Psi\rangle$, is given by

$$\begin{aligned}E_V[\Psi] &= \langle\Psi|\hat{H}_V|\Psi\rangle \\ &= -V \sum_{\langle ij\rangle} \sum_{\sigma\sigma'} \langle \hat{n}_{i\sigma}\hat{n}_{j\sigma'}\rangle \\ &= \underbrace{-V \sum_{\langle ij\rangle} \sum_{\sigma} \langle \hat{n}_{i\sigma}\hat{n}_{j\sigma}\rangle}_{\text{s.s.}} \underbrace{-V \sum_{\langle ij\rangle} \sum_{\sigma} \langle \hat{n}_{i\sigma}\hat{n}_{j\overline{\sigma}}\rangle}_{\text{o.s.}}\end{aligned} \tag{2.5}$$

[1] Extensions to finite temperatures is simple: minimization must be carried out on free energy, while expectation values must be taken in a thermodynamic fashion.

Shorthand notation has been used: $\langle\Psi|\cdot|\Psi\rangle = \langle\cdot\rangle$. The ground-state must realize the condition

$$\frac{\delta}{\delta\langle\Psi|}E[\Psi] = 0$$

being $E[\Psi]$ the total energy (made up of the three terms of couplings t, U and V).

[Expand derivation.]

The functional derivative must be carried out in a variational fashion including a Lagrange multiplier, the latter accounting for state-norm conservation, as is done normally in deriving the Hartree-Fock approximation for the eigenenergies of the electron liquid [4, 5].

Opposite-spin terms. Consider first the o.s. terms of Eq. (2.5): take e.g. the term $\hat{n}_{i\uparrow}\hat{n}_{i+\delta_x\downarrow}$. As in Eq. (2.2), Wick's Theorem states that, if the expectation value is performed onto a coherent state,

$$\begin{aligned}\langle\hat{n}_{i\uparrow}\hat{n}_{i+\delta_x\downarrow}\rangle &= \langle\hat{c}^\dagger_{i\uparrow}\hat{c}^\dagger_{i+\delta_x\downarrow}\hat{c}_{i+\delta_x\downarrow}\hat{c}_{i\uparrow}\rangle \\ &= \underbrace{\langle\hat{c}^\dagger_{i\uparrow}\hat{c}^\dagger_{i+\delta_x\downarrow}\rangle\langle\hat{c}_{i+\delta_x\downarrow}\hat{c}_{i\uparrow}\rangle}_{\text{Cooper}} - \underbrace{\langle\hat{c}^\dagger_{i\uparrow}\hat{c}_{i+\delta_x\downarrow}\rangle\langle\hat{c}^\dagger_{i+\delta_x\downarrow}\hat{c}_{i\uparrow}\rangle}_{\text{Fock}} + \underbrace{\langle\hat{c}^\dagger_{i\uparrow}\hat{c}_{i\uparrow}\rangle\langle\hat{c}^\dagger_{i+\delta_x\downarrow}\hat{c}_{i+\delta_x\downarrow}\rangle}_{\text{Hartree}}\end{aligned}$$

Identical decompositions are given for all others NNs. Of the three terms above:

- The Coooper term breaks $\mathrm{U}^{\mathrm{c}}(1)$ charge symmetry, allowing for supeconducting instabilities;
- The Fock term breaks the $\mathrm{U}^z(1)$ symmetry, because it accounts for a site hop *plus* spin flip process;
- The Hartree term breaks translational invariance, because the mean-field to interact with is given by the local density. SU(2) symmetry is also broken, because we do not have spin DoF perfect degeneracy anymore, but $\mathrm{U}^z(1$ symmetry still holds.

Then, to look for AF instability only the Hartree term is to be accounted; instead, in superconducting instability only the Cooper term contributes. Note that for superconducting instabilities, due to superexchange mechanism (as explained in App. **??**) the o.s. term account for singlet pairing as well as zero-spin triplet pairing. Which channel is preferred, is a matter of thermodynamic advantage.

Same-spin terms. Consider then the same-spin terms: take e.g. the term $\hat{n}_{i\uparrow}\hat{n}_{i+\delta_x\uparrow}$. As above,

$$\begin{aligned}\langle\hat{n}_{i\uparrow}\hat{n}_{i+\delta_x\uparrow}\rangle &= \langle\hat{c}^\dagger_{i\uparrow}\hat{c}^\dagger_{i+\delta_x\uparrow}\hat{c}_{i+\delta_x\uparrow}\hat{c}_{i\uparrow}\rangle \\ &= \underbrace{\langle\hat{c}^\dagger_{i\uparrow}\hat{c}^\dagger_{i+\delta_x\uparrow}\rangle\langle\hat{c}_{i+\delta_x\uparrow}\hat{c}_{i\uparrow}\rangle}_{\text{Cooper}} - \underbrace{\langle\hat{c}^\dagger_{i\uparrow}\hat{c}_{i+\delta_x\uparrow}\rangle\langle\hat{c}^\dagger_{i+\delta_x\uparrow}\hat{c}_{i\uparrow}\rangle}_{\text{Fock}} + \underbrace{\langle\hat{c}^\dagger_{i\uparrow}\hat{c}_{i\uparrow}\rangle\langle\hat{c}^\dagger_{i+\delta_x\uparrow}\hat{c}_{i+\delta_x\uparrow}\rangle}_{\text{Hartree}}\end{aligned}$$

Identical consideration as in the above paragraph hold for each term. The only difference with the o.s. terms is given by the Fock term: since the spin-flip process is absent, now the Fock fluctuations actually contribute as an effective NN hopping term. In other words, this term does not break $\mathrm{U}^z(1)$ symmetry and thus is perfectly legitimate, say, in AF or superconducting phase. As a final remark, notice that the superconducting instabilities of the s.s. terms account only for triplet pairing. The only possible superconducting ordering established by the means of these terms is odd in real space. Then s-wave and d-wave superconductivity cannot establish in this channel; p_ℓ-wave superconductivity, instead, can.

2.2.2 Reciprocal space transform of the model interactions

It is useful to derive analytically the reciprocal-space form of both the U and V interactions. Let us start from the latter.

Non-local attraction. Consider a generic bond, say, the one connecting sites j and $j \pm \delta_\ell$ (variable i is here referred to as the imaginary unit to avoid confusion). $\mathbf{x}_j$ is the 2D notation for the position of site j, while $\boldsymbol{\delta}_\ell$ is the 2D notation for the lattice spacing previously indicated as δ_ℓ. Fourier transform it according to the convention

$$\hat{c}_{j\sigma} = \frac{1}{\sqrt{L_x L_y}} \sum_{\mathbf{k}\in \mathrm{BZ}} e^{-i\mathbf{k}\cdot\mathbf{x}_j} \hat{c}_{\mathbf{k}\sigma}$$

Then:

$$\begin{aligned}\hat{n}_{j\sigma}\hat{n}_{j\pm\delta_\ell\sigma'} &= \hat{c}^\dagger_{j\sigma}\hat{c}^\dagger_{j\pm\delta_\ell\sigma'}\hat{c}_{j\pm\delta_\ell\sigma'}\hat{c}_{j\sigma} \\ &= \frac{1}{(L_xL_y)^2}\sum_{\nu=1}^{4}\sum_{\mathbf{k}_\nu\in\mathrm{BZ}} e^{i[(\mathbf{k}_1+\mathbf{k}_2)-(\mathbf{k}_3+\mathbf{k}_4)]\cdot\mathbf{x}_j} e^{\pm i(\mathbf{k}_2-\mathbf{k}_3)\cdot\boldsymbol{\delta}_\ell} \hat{c}^\dagger_{\mathbf{k}_1\sigma}\hat{c}^\dagger_{\mathbf{k}_2\sigma'}\hat{c}_{\mathbf{k}_3\sigma'}\hat{c}_{\mathbf{k}_4\sigma}\end{aligned}$$

Then, the interaction at site j, spin σ with its NNs at spin σ' – indicated as $(j\sigma\sigma')$ – is given by

$$\begin{aligned}(j\sigma\sigma') &= -V\sum_{\ell=x,y}\sum_{\delta=\pm\delta_\ell}\hat{n}_{j\sigma}\hat{n}_{j\pm\delta_\ell\sigma'} \\ &= -\frac{V}{(L_xL_y)^2}\sum_{\ell=x,y}\sum_{\nu=1}^{4}\sum_{\mathbf{k}_\nu\in\mathrm{BZ}} e^{i[(\mathbf{k}_1+\mathbf{k}_2)-(\mathbf{k}_3+\mathbf{k}_4)]\cdot\mathbf{x}_j} \\ &\qquad\qquad \times\left(e^{i(\mathbf{k}_2-\mathbf{k}_3)\cdot\boldsymbol{\delta}_\ell}+e^{-i(\mathbf{k}_2-\mathbf{k}_3)\cdot\boldsymbol{\delta}_\ell}\right)\hat{c}^\dagger_{\mathbf{k}_1\sigma}\hat{c}^\dagger_{\mathbf{k}_2\sigma'}\hat{c}_{\mathbf{k}_3\sigma'}\hat{c}_{\mathbf{k}_4\sigma} \\ &= -\frac{2V}{(L_xL_y)^2}\sum_{\ell=x,y}\sum_{\nu=1}^{4}\sum_{\mathbf{k}_\nu\in\mathrm{BZ}} e^{i[(\mathbf{k}_1+\mathbf{k}_2)-(\mathbf{k}_3+\mathbf{k}_4)]\cdot\mathbf{x}_j}\cos\left[(\mathbf{k}_2-\mathbf{k}_3)\cdot\boldsymbol{\delta}_\ell\right]\hat{c}^\dagger_{\mathbf{k}_1\sigma}\hat{c}^\dagger_{\mathbf{k}_2\sigma'}\hat{c}_{\mathbf{k}_3\sigma'}\hat{c}_{\mathbf{k}_4\sigma}\end{aligned}$$

The full non-local interaction is given by summing over all sites of $\mathcal{S}_a$ (which is, half the sites of $\mathcal{S}$). This gives back momentum conservation,

$$\frac{1}{L_xL_y}\sum_{j\in\mathcal{S}_a} e^{i[(\mathbf{k}_1+\mathbf{k}_2)-(\mathbf{k}_3+\mathbf{k}_4)]\cdot\mathbf{x}_j} = \frac{1}{2}\delta_{\mathbf{k}_1+\mathbf{k}_2=\mathbf{k}_3+\mathbf{k}_4}$$

Let $\mathbf{k}_1+\mathbf{k}_2=\mathbf{k}_3+\mathbf{k}_4=\mathbf{K}$, and define $\mathbf{k}$, $\mathbf{k}'$ such that

$$\mathbf{k}_1 \equiv \mathbf{K}+\mathbf{k} \qquad \mathbf{k}_2 \equiv \mathbf{K}-\mathbf{k} \qquad \mathbf{k}_3 \equiv \mathbf{K}-\mathbf{k}' \qquad \mathbf{k}_4 \equiv \mathbf{K}+\mathbf{k}' \qquad \delta\mathbf{k} \equiv \mathbf{k}-\mathbf{k}'$$

Sums over these variables must be intended as over the Brillouin Zone (BZ). Then, finally

$$\begin{aligned}\hat{H}_V &= \sum_{j\in\mathcal{S}_a}\sum_{\sigma\sigma'}(j\sigma\sigma') \\ &= -\frac{V}{L_xL_y}\sum_{\sigma\sigma'}\sum_{\ell=x,y}\sum_{\mathbf{K},\mathbf{k},\mathbf{k}'}\cos\left(\delta\mathbf{k}\cdot\boldsymbol{\delta}_\ell\right)\hat{c}^\dagger_{\mathbf{K}+\mathbf{k}\sigma}\hat{c}^\dagger_{\mathbf{K}-\mathbf{k}\sigma'}\hat{c}_{\mathbf{K}-\mathbf{k}'\sigma'}\hat{c}_{\mathbf{K}+\mathbf{k}'\sigma} \\ &= -\frac{V}{L_xL_y}\sum_{\sigma\sigma'}\sum_{\mathbf{K},\mathbf{k},\mathbf{k}'}\left[\cos\left(\delta k_x\right)+\cos\left(\delta k_y\right)\right]\hat{c}^\dagger_{\mathbf{K}+\mathbf{k}\sigma}\hat{c}^\dagger_{\mathbf{K}-\mathbf{k}\sigma'}\hat{c}_{\mathbf{K}-\mathbf{k}'\sigma'}\hat{c}_{\mathbf{K}+\mathbf{k}'\sigma} \qquad (2.6)\end{aligned}$$

The result here obtained will be used various times in next chapters. Note that different Wick contraction schemes lead to different results:

$$\overbrace{c^\dagger_{\mathbf{K}+\mathbf{k}\sigma}c^\dagger_{\mathbf{K}-\mathbf{k}\sigma'}}c_{\mathbf{K}-\mathbf{k}'\sigma'}c_{\mathbf{K}+\mathbf{k}'\sigma} \qquad \text{Cooper contraction} \qquad (2.7)$$

$$\overbrace{c^\dagger_{\mathbf{K}+\mathbf{k}\sigma}c^\dagger_{\mathbf{K}-\mathbf{k}\sigma'}c_{\mathbf{K}-\mathbf{k}'\sigma'}}c_{\mathbf{K}+\mathbf{k}'\sigma} \qquad \text{Fock contraction} \qquad (2.8)$$

$$\overbrace{c^\dagger_{\mathbf{K}+\mathbf{k}\sigma}c^\dagger_{\mathbf{K}-\mathbf{k}\sigma'}c_{\mathbf{K}-\mathbf{k}'\sigma'}c_{\mathbf{K}+\mathbf{k}'\sigma}} \qquad \text{Hartree contraction} \qquad (2.9)$$

which will be used explicitly later on.

Local repulsion. A somewhat identical argument can be carried out for the local interaction,

$$\hat{H}_U = U \sum_{i \in \mathcal{S}} \hat{n}_{i\uparrow} \hat{n}_{i\downarrow}$$

The only difference here is made by the fact that the interaction is repulsive on-site, thus the final structure factor in the Fourier transform disappears as well as the minus sign,

$$\hat{H}_U = \frac{U}{L_x L_y} \sum_{\mathbf{K},\mathbf{k},\mathbf{k}'} \hat{c}^\dagger_{\mathbf{K}+\mathbf{k}\uparrow} \hat{c}^\dagger_{\mathbf{K}-\mathbf{k}\downarrow} \hat{c}_{\mathbf{K}-\mathbf{k}'\downarrow} \hat{c}_{\mathbf{K}+\mathbf{k}'\uparrow} \tag{2.10}$$

When contracting these fermionic operators, identical considerations as for the non-local counterpart (2.6) hold.

2.3 General computational approach to MFT

The general sketch of a self-consistent Hartree-Fock algorithm in our context is simple enough. Start from a fermionic quartic hamiltonian,

$$\hat{H} = \sum_{\alpha\beta} A_{\alpha\beta} \hat{c}^\dagger_\alpha \hat{c}_\beta + \sum_{\alpha\beta\gamma\delta} B_{\alpha\beta\gamma\delta} \hat{c}^\dagger_\alpha \hat{c}^\dagger_\beta \hat{c}_\gamma \hat{c}_\delta + \text{h.c.} \tag{2.11}$$

where $A_{\alpha\beta}$, $B_{\alpha\beta\gamma\delta}$ are model parameters. We limit ourselves to quartic hamiltonians, but the idea can be extended. As discussed before, in this kind of context MFT is employed by applying Wick's theorem. This way, the quartic hamiltonian is effectively reduced to a quadratic hamiltonian,

$$\hat{H} \simeq \hat{H}^{(\text{eff})} = \sum_{\alpha\beta} C_{\alpha\beta} \hat{c}^\dagger_\alpha \hat{c}_\beta + \sum_{\alpha\beta} D_{\alpha\beta} \hat{c}^\dagger_\alpha \hat{c}^\dagger_\beta + \text{h.c.} \tag{2.12}$$

where now the new parameters, which we will refer to as Hartree-Fock parameters (HFP), depend on the model itself via the equations

$$C_{\alpha\beta} = A_{\alpha\beta} + \sum_{\gamma\delta} \left[B_{\alpha\gamma\delta\beta} - B_{\alpha\gamma\beta\delta} \right] \langle \hat{c}^\dagger_\gamma \hat{c}_\delta \rangle$$

$$D_{\alpha\beta} = \sum_{\gamma\delta} B_{\alpha\beta\gamma\delta} \langle \hat{c}_\gamma \hat{c}_\delta \rangle$$

These equations are determined by many-body expectation values, which in general are computed by the means of thermal averages over the lowest energy density matrix. A self consistent Hartree-Fock scheme goes as follows;

1. Apply MFT to the quartic hamiltonian, recovering its general theoretic effective form;
2. Impose selection rules on the parameters $C_{\alpha\beta}$, $D_{\alpha\beta}$, eventually eliminating those not respecting the symmetry sector we are working in[2];
3. Choose a starting value and a coherent symmetry structure for the remaining parameters;
4. Enter iterative scheme of Fig. 2.2:
   a) Diagonalize the effective hamiltonian $\hat{H}^{(\text{eff})}[C, D]$ and recover the ground-state $|\Psi[C, D]\rangle$;
   b) Compute the new parameters $C'_{\alpha\beta}$, $D'_{\alpha\beta}$ via the self consistent equations;
   c) Initialize the new effective hamiltonian $\hat{H}^{(\text{eff})}[C', D']$ and repeat the cycle until convergence.

Of course, to work any of these algorithms we need to know how to diagonalize the hamiltonian. In the context of the Extended Hubbad Model at thermal equilibrium, due to the phases we are simulating, we know analytically the diagonalized hamiltonian, and making use of this knowledge we are able to reduce the self consistent scheme to a simple iterative algorithm. An explicit example of HF algorithm used in present text, somewhat simplified due to the presence of a single HF parameter, is given in App. **??**.

[2] As an example: if we choose not to break charge conservation, set $\forall \alpha, \beta : \; D_{\alpha\beta} = 0$.

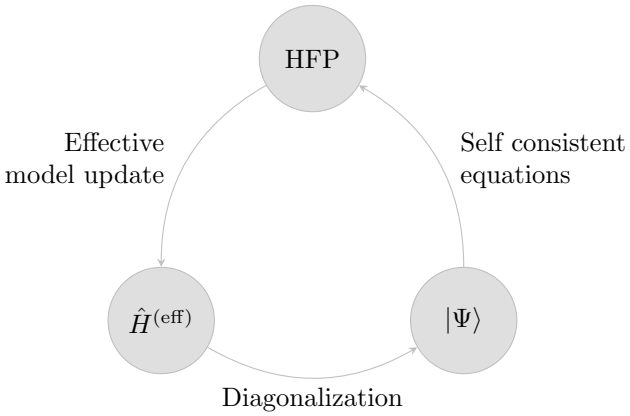

Figure 2.2 Schematization of the self-consistent Hartree Fock method described in Sec. 2.3. The effective model is solved, the solution is used to estimate self-consistently the Hartree Fock vector, which is then used to update iteratively the model itself.

2.3.1 Square lattice spatial symmetry structures

When dealing with phases which respect translational symmetry, or at most reduce it to a weaker symmetry by shrinking the Brillouin Zone, it' useful to work in reciprocal space, as discussed in Sec. 3.3. This is the case for the two competing phases explored in next chapters: antiferromagnetic and superconducting. A particular phase can show specific spatial symmetries, and so will the Hartree Fock parameters. The key point to notice is that self-consistent equations involve sums (or integrals) to be computed over fermionic states, which can be heavily simplified by employing said symmetries.

For the 2D square lattice, various spatial symmetries are possible. [To be continued...]

2.3.2 Symmetry-based optimizations

[To be continued...]

Chapter 3

Superconducting instability

This chapter is devoted to studying the superconducting phase of the system. The only symmetry we assume to break is the $\mathrm{U}^{\mathrm{c}}(1)$ charge symmetry, thus allowing for superconducting fluctuations. As is described thoroughly in Sec. **??**, the hopping amplitude is renormalized because of the non-local attraction. The symmetry structure of the pairing mechanism determines the contributing Cooper fluctuations: for s-wave and d-wave superconductivity, only the o.s. Cooper term contributes; for p_ℓ-wave superconductivity, the s.s. term contributes as well. In the following sections, a derivation containing both Cooper terms is proposed.

[To be continued: separate singlet and triplet pairing channels, and describe them separately by the means of four-components Nambu spinors. Use selection rules to set $\Delta^{(p_\ell)} = 0$ in the singlet channel, in order to justify results obtained by a pure space-even simulation containing just the o.s. terms.]

3.1 Cooper fluctuations in the EHM

Let us start once again from the general EHM of Eq. (1.2),

$$\hat{H} = \underbrace{-t \sum_{\langle ij \rangle} \sum_{\sigma} \hat{c}^\dagger_{i\sigma} \hat{c}_{j\sigma}}_{\hat{H}_t} \underbrace{+U \sum_{i} \hat{c}^\dagger_{i\uparrow} \hat{c}^\dagger_{i\downarrow} \hat{c}_{i\downarrow} \hat{c}_{i\uparrow}}_{\hat{H}_U} \underbrace{-V \sum_{\langle ij \rangle} \sum_{\sigma\sigma'} \hat{c}^\dagger_{i\sigma} \hat{c}^\dagger_{j\sigma'} \hat{c}_{j\sigma'} \hat{c}_{i\sigma}}_{\hat{H}_V}$$

As is discussed in Sec. 2.2, when applying Wick's theorem the resulting terms break the natural symmetries of the model. The superconducting symmetry we study breaks just the $\mathrm{U}^{\mathrm{c}}(1)$ charge conservation. Now, when dealing with superconducting Cooper pairing we need to account also for the spatial structure of the Cooper pair itself. Consider the generic Cooper fluctuation

$$\langle \hat{c}^\dagger_{i\sigma} \hat{c}^\dagger_{j\sigma'} \rangle \quad \text{with } i, j \text{ NN}$$

From basic Quantum Mechanics we know the summation rules of the spin algebra $\mathfrak{su}(2)$,

$$\frac{1}{2} \otimes \frac{1}{2} = 0 \oplus 1$$

The two pairing channels are, at this level, the singlet channel associated to total spin 0 and the triplet channel associated to total spin 1. If we impose a specific spatial symmetry on the hamiltonian the ground state wavefunction will follow naturally, and the pairing channel will be the one providing a total anti-symmetry to the full wavefunction. This gives a selection rule over the relevant pairings: if we work with space symmetric structures – say, s^*-wave or d-wave – the pairing will happen in singlet channel, allowing us to eliminate the triplet pairing. This concept is summarized in Tab. 3.1.

[Add: Cooper pairing considerations in the pure Hubbard model.]

3.2 Singlet pairing

This section deals with singlet pairing superconductivity, somewhat the simplest form of Cooper pairing. Considering Cooper fluctuations in the singlet channel, we need to break $\mathrm{U}^{c}(1)$ symmetry

Spatial structure	Pairing channel	Relevant pairing
Symmetric wave function	Singlet pairing	Just $\langle \hat{c}^\dagger_{i\sigma}\hat{c}^\dagger_{j\bar{\sigma}}\rangle$
Anti-symmetric wave function	Triplet pairing	Both $\langle \hat{c}^\dagger_{i\sigma}\hat{c}^\dagger_{j\bar{\sigma}}\rangle$ and $\langle \hat{c}^\dagger_{i\sigma}\hat{c}^\dagger_{j\sigma}\rangle$

Table 3.1 | Relation of the Cooper pairing channell with the wavefunction spatial symmetry (intended as the inversion $(x, y) \to (-x, -y)$).

imposing space inversion symmetry. Let us now break down the MFT discussion for the local and non-local interactions.

Local interaction U. Consider first the local part,

$$\hat{H}_U = U\sum_{i\in\mathcal{S}} \hat{n}_{i\uparrow}\hat{n}_{i\downarrow} \simeq U\sum_{i\sigma}\Big[\langle \hat{c}^\dagger_{i\uparrow}\hat{c}^\dagger_{i\downarrow}\rangle \hat{c}_{i\downarrow}\hat{c}_{i\uparrow} + \hat{c}^\dagger_{i\uparrow}\hat{c}^\dagger_{i\downarrow}\langle \hat{c}_{i\downarrow}\hat{c}_{i\uparrow}\rangle\Big]$$

and use the result of Eq. (2.10),

$$\hat{H}_U \simeq \frac{U}{L_xL_y}\sum_{\mathbf{K},\mathbf{k},\mathbf{k}'}\Big[\langle \hat{c}^\dagger_{\mathbf{K}+\mathbf{k}\uparrow}\hat{c}^\dagger_{\mathbf{K}-\mathbf{k}\downarrow}\rangle \hat{c}_{\mathbf{K}-\mathbf{k}'\downarrow}\hat{c}_{\mathbf{K}+\mathbf{k}'\uparrow} + \hat{c}^\dagger_{\mathbf{K}+\mathbf{k}\uparrow}\hat{c}^\dagger_{\mathbf{K}-\mathbf{k}\downarrow}\langle \hat{c}_{\mathbf{K}-\mathbf{k}'\downarrow}\hat{c}_{\mathbf{K}+\mathbf{k}'\uparrow}\rangle\Big]$$

We are not breaking translational invariance, thus only Cooper fluctuations with net zero total momentum are allowed. This means only $\mathbf{K} = \mathbf{0}$ contributes. Define the pairing operator

$$\hat{\phi}_{\mathbf{k}} \equiv \hat{c}_{-\mathbf{k}\downarrow}\hat{c}_{\mathbf{k}\uparrow} \qquad \hat{\phi}^\dagger_{\mathbf{k}} \equiv \hat{c}^\dagger_{\mathbf{k}\uparrow}\hat{c}^\dagger_{-\mathbf{k}\downarrow}$$

Then the non local repulsion reduces to the ordinary BCS-like interaction,

$$\hat{H}_U \simeq \sum_{\mathbf{k}}\Big[\mathcal{U}_{\mathbf{k}}\hat{\phi}_{\mathbf{k}} + \mathcal{U}^*_{\mathbf{k}}\hat{\phi}^\dagger_{\mathbf{k}}\Big] \quad \text{where} \quad \mathcal{U}_{\mathbf{k}} \equiv \frac{U}{L_xL_y}\sum_{\mathbf{k}}\langle \hat{\phi}^\dagger_{\mathbf{k}}\rangle \tag{3.1}$$

Note that $\mathcal{U}_{\mathbf{k}}$ is actually momentum independent. This is due to the fact that the repulsion is completely localized.

Non-local interaction V. Consider now the non-local term, [To be continued. . .]This approach leads to the conclusion that the (coherent) ground-state of the system must be an eigenstate of the mean-field effective hamiltonian:

$$\begin{aligned}\hat{H}^{(\mathrm{e})} = &-t\sum_{\langle ij\rangle}\sum_{\sigma}\hat{c}^\dagger_{i\sigma}\hat{c}_{j\sigma} + U\sum_{i\in\mathcal{S}}\hat{n}_{i\uparrow}\hat{n}_{i\downarrow} \\ &- V\sum_{i\in\mathcal{S}}\sum_{\ell=x,y}\sum_{\delta=\pm\delta_\ell}\Big[\langle \hat{c}^\dagger_{i\uparrow}\hat{c}^\dagger_{i+\delta\downarrow}\rangle \hat{c}_{i+\delta\downarrow}\hat{c}_{i\uparrow} + \text{h.c.}\Big]\end{aligned} \tag{3.2}$$

Note that I am here summing over $i \in \mathcal{S}$: this is the same as considering both the $\uparrow\downarrow$ *plus* the $\downarrow\uparrow$ terms of the o.s. hamiltonian involved in even-wave pairing. The pairing correlation function is defined across each bond as the pairing expectation

$$g_{ij} \equiv \langle \hat{c}^\dagger_{i\uparrow}\hat{c}^\dagger_{j\downarrow}\rangle$$

The effective hamiltonian reads:

$$\hat{H}^{(\mathrm{e})} = -t\sum_{\langle ij\rangle}\sum_{\sigma}\hat{c}^\dagger_{i\sigma}\hat{c}_{j\sigma} + U\sum_{i\in\mathcal{S}}\hat{n}_{i\uparrow}\hat{n}_{i\downarrow} - V\sum_{\langle ij\rangle}\Big[g_{ij}\hat{c}_{j\downarrow}\hat{c}_{i\uparrow} + g^*_{ij}\hat{c}^\dagger_{i\uparrow}\hat{c}^\dagger_{j\downarrow}\Big] \tag{3.3}$$

As in standard BCS theory, this hamiltonian – being quadratic in the electronic operators – can be diagonalized via a Bogoliubov rotation. Superconducting pairing can arise both from the local U term and from the non-local V term. In next sections it is assumed the V term generates dominant superconductivity via its weak non-local pairing.

3.2.1 Mean-field treatment of the local term

The mean-field description of the local (on-site) U interaction is given in detail in App. **??**, along with a simple numerical analysis of the insurgence of antiferromagnetic ordering in a Hartree-Fock approximation scheme. Here the Cooper pairing is likewise assumed to dominate. Performing an analysis analogous to the one carried out in last section, we get the decoupling

$$U\sum_{i\in\mathcal{S}}\hat{n}_{i\uparrow}\hat{n}_{i\downarrow}\simeq U\sum_{i\sigma}\left[f_i\hat{c}_{i\downarrow}\hat{c}_{i\uparrow}+f_i^*\hat{c}_{i\uparrow}^\dagger\hat{c}_{i\downarrow}^\dagger\right]$$

being

$$f_i\equiv\langle\hat{c}_{i\uparrow}^\dagger\hat{c}_{i\downarrow}^\dagger\rangle$$

Collect f and g in the unique function of two variables:

$$C(i,j)=\begin{cases}f_i & \text{if}\quad i=j\\ g_{ij} & \text{if}\quad |i-j|=1\\ (\cdots) & \text{otherwise}\end{cases}$$

which expresses the generic correlator $\langle\hat{c}_{i\uparrow}^\dagger\hat{c}_{j\downarrow}^\dagger\rangle$. The correlator for $|i-j|>1$ is left unexpressed, and supposed to be subdominant. The decoupled hamiltonian, apart from pure energy shifts and suppressed terms, is given by

$$\begin{aligned}\hat{H}^{(\mathrm{e})}=-t\sum_{\langle ij\rangle}\sum_{\sigma}\hat{c}_{i\sigma}^\dagger\hat{c}_{j\sigma}+U\sum_i\left[f_i\hat{c}_{i\downarrow}\hat{c}_{i\uparrow}+f_i^*\hat{c}_{i\uparrow}^\dagger\hat{c}_{i\downarrow}^\dagger\right]\\ -V\sum_{\langle ij\rangle}\left[g_{ij}\hat{c}_{j\downarrow}\hat{c}_{i\uparrow}+g_{ij}^*\hat{c}_{i\uparrow}^\dagger\hat{c}_{j\downarrow}^\dagger\right]\end{aligned}\tag{3.4}$$

Next section is devoted to analyzing the consequences of choosing a specific topology (which is, symmetry structure) for the pairing correlations.

3.2.2 Topological correlations

Topology plays an important role in establishing SC, giving rise to anisotropic pairing as well as real space structures for the Cooper pairs. The correlator g_{ij} is a function of position, specifically of its variables difference $\boldsymbol{\delta}\equiv\mathbf{x}_j-\mathbf{x}_i$. Over the square lattice with NN interaction, the latter can assume four values: $\boldsymbol{\delta}=\pm\boldsymbol{\delta}_x,\pm\boldsymbol{\delta}_y$. For a function of space defined over the four rim sites $\mathbf{x}_i\pm\boldsymbol{\delta}_\ell$ of Fig. 2.1, various symmetry structures can be defined under the planar rotations group SO(2). In other words, the function $g_{\boldsymbol{\delta}}$ can be decomposed in planar harmonics (which are simply the sine-cosine basis). Equivalently, given two NN sites i, j

$$g_{ij}=\sum_\gamma g^{(\gamma)}\varphi_{ij}^{(\gamma)}$$

where $g^{(\gamma)}$ are the g_{ij} symmetries-decomposition coefficients while $\varphi_{ij}^{(\gamma)}$ are the form factors listed in Tab. 3.2, a simple orthonormal rearrangement of the harmonics basis.

SC is established with a given symmetry – which means, symmetry breaking in the phase transition proceeds in a specific channel. Conventional BCS superconductivity arises from the only possible spatial structure of the local pairing, s-wave – here appearing as a local term (Fig. 3.1a) and extended on a non-local term (Fig. 3.1b). Cuprates exhibit a tendency towards $d_{x^2-y^2}$ SC, while other materials towards p-wave types – eventually with some chirality, as is the case for $p_x\pm ip_y$ SCs. To establish SC under a certain symmetry γ means that Cooper pairs acquire said symmetry – which implies, for correlations, $g^{(\gamma')}=g^{(\gamma)}\delta_{\gamma\gamma'}$. and $g_{ij}\propto\varphi_{ij}^{(\gamma)}$.

3.3 Mean-Field theory reciprocal space description

In this BCS-like approach, a self-consistent equation for the gap function must be retrieved in order to further investigate the model and extract the conditions for the formation of a superconducting phase with a given pairing topology. In order to do so, let me take a step back and perform explicitly the Fourier-transform of the various terms of Eq. 1.2.

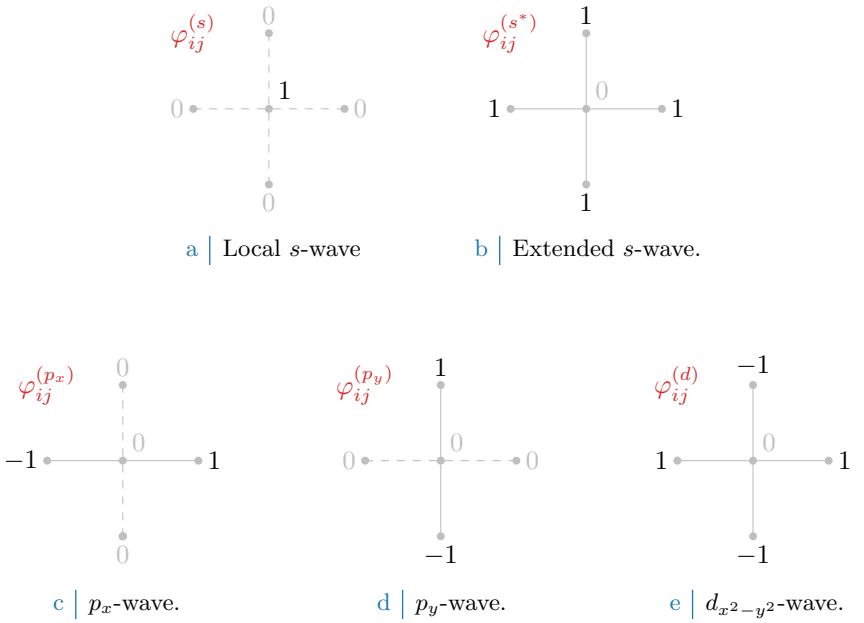

a | Local s-wave b | Extended s-wave.

c | p_x-wave. d | p_y-wave. e | $d_{x^2-y^2}$-wave.

Figure 3.1 | Form factors at different topologies, as listed in Tab. 3.2. In figures five sites are represented: the hub site i and its four NN. Solid lines represent non-zero values for $\varphi_{\boldsymbol{\delta}}$, while dashed lines represent vanishing factors.

Structure	Form factor	Graph
s-wave	$\varphi_{ij}^{(s)} = \delta_{ij}$	Fig. 3.1a
Extended s-wave	$\varphi_{ij}^{(s^*)} = \delta_{j=i+\delta_x} + \delta_{j=i-\delta_x} + \delta_{j=i+\delta_y} + \delta_{j=i-\delta_y}$	Fig. 3.1b
p_x-wave	$\varphi_{ij}^{(p_x)} = \delta_{j=i+\delta_x} - \delta_{j=i-\delta_x}$	Fig. 3.1c
p_y-wave	$\varphi_{ij}^{(p_y)} = \delta_{j=i+\delta_y} - \delta_{j=i-\delta_y}$	Fig. 3.1d
$d_{x^2-y^2}$-wave	$\varphi_{ij}^{(d)} = \delta_{j=i+\delta_x} + \delta_{j=i-\delta_x} - \delta_{j=i+\delta_y} - \delta_{j=i-\delta_y}$	Fig. 3.1e

Table 3.2 | First four spatial structures for the correlation function $C(i,j)$. In the middle column, all spatial dependence is included in the δs, while $f^s, g^{(\gamma)} \in \mathbb{C}$. The last column indicates the graph representation of each contribution given in Fig. **??**. Subscript $x^2 - y^2$ is omitted for notational clarity.

3.3.1 Kinetic term

The kinetic part is trivial to transform. The followed convention is

$$\hat{c}_{j\sigma} = \frac{1}{\sqrt{L_x L_y}} \sum_{\mathbf{k}\in \mathrm{BZ}} e^{-i\mathbf{k}\cdot\mathbf{x}_j} \hat{c}_{\mathbf{k}\sigma}$$

Calculation is carried out in App. **??**. Let

$$\epsilon_{\mathbf{k}} \equiv -2t\left[\cos(k_x\delta_x) + \cos(k_y\delta_y)\right]$$

then we have

$$\begin{aligned} -t\sum_{\langle ij\rangle}\sum_{\sigma} \hat{c}_{i\sigma}^{\dagger}\hat{c}_{j\sigma} &= \sum_{\mathbf{k}\sigma} \epsilon_{\mathbf{k}} \hat{c}_{\mathbf{k}\sigma}^{\dagger}\hat{c}_{\mathbf{k}\sigma} \\ &= \sum_{\mathbf{k}} \epsilon_{\mathbf{k}} \left[\hat{c}_{\mathbf{k}\uparrow}^{\dagger}\hat{c}_{\mathbf{k}\uparrow} + \hat{c}_{\mathbf{k}\downarrow}^{\dagger}\hat{c}_{\mathbf{k}\downarrow}\right] \\ &= \sum_{\mathbf{k}} \epsilon_{\mathbf{k}} \left[\hat{c}_{\mathbf{k}\uparrow}^{\dagger}\hat{c}_{\mathbf{k}\uparrow} - \hat{c}_{-\mathbf{k}\downarrow}\hat{c}_{-\mathbf{k}\downarrow}^{\dagger}\right] \end{aligned}$$

In last passage I used fermionic anti-commutation rules and reversed the sign of the mute variable. This will become useful later.

3.3.2 Non-local attraction

Consider now the result of Eq. (2.6). Taking in the mean-field approximation (with Cooper pair symmetry breaking), we get

$$\hat{c}^\dagger_{\mathbf{K}+\mathbf{k}\uparrow}\hat{c}^\dagger_{\mathbf{K}-\mathbf{k}\downarrow}\hat{c}_{\mathbf{K}-\mathbf{k}'\downarrow}\hat{c}_{\mathbf{K}+\mathbf{k}'\uparrow} \simeq \langle\hat{c}^\dagger_{\mathbf{K}+\mathbf{k}\uparrow}\hat{c}^\dagger_{\mathbf{K}-\mathbf{k}\downarrow}\rangle\hat{c}_{\mathbf{K}-\mathbf{k}'\downarrow}\hat{c}_{\mathbf{K}+\mathbf{k}'\uparrow} + \hat{c}^\dagger_{\mathbf{K}+\mathbf{k}\uparrow}\hat{c}^\dagger_{\mathbf{K}-\mathbf{k}\downarrow}\langle\hat{c}_{\mathbf{K}-\mathbf{k}'\downarrow}\hat{c}_{\mathbf{K}+\mathbf{k}'\uparrow}\rangle + \cdots$$

Take e.g. $\langle\hat{c}^\dagger_{\mathbf{K}+\mathbf{k}\uparrow}\hat{c}^\dagger_{\mathbf{K}-\mathbf{k}\downarrow}\rangle$: the only non-zero contribution can come from the $\mathbf{K}=\mathbf{0}$ term, as will be discussed self-consistently in Sec. 3.3.5. Then finally:

$$\hat{H}_V \simeq -\sum_{\mathbf{k},\mathbf{k}'} V_{\mathbf{k}\mathbf{k}'}\left[\langle\hat{\phi}^\dagger_{\mathbf{k}}\rangle\hat{\phi}_{\mathbf{k}'} + \langle\hat{\phi}_{\mathbf{k}}\rangle\hat{\phi}^\dagger_{\mathbf{k}'}\right]$$

having I defined the two-body potential

$$V_{\mathbf{k}\mathbf{k}'} = \frac{2V}{L_xL_y}\left[\cos\left(\delta k_x\delta_x\right) + \cos\left(\delta k_y\delta_y\right)\right]$$

Now, consider the term

$$\cos\left(\delta k_x\right) + \cos\left(\delta k_y\right) = \cos k_x\cos k'_x + \sin k_x\sin k'_x + \cos k_y\cos k'_y + \sin k_y\sin k'_y$$

For the sake of readability, the notations

$$c_\ell \equiv \cos k_\ell \qquad s_\ell \equiv \sin k_\ell \qquad c'_\ell \equiv \cos k'_\ell \qquad s'_\ell \equiv \sin k'_\ell$$

are used. Group the four terms above,

$$\underbrace{\left(c_xc'_x + c_yc'_y\right)}_{\text{Symmetric}} + \underbrace{\left(s_xs'_x + s_ys'_y\right)}_{\text{Anti-symmetric}} \tag{3.5}$$

The first two exhibit inversion symmetry for both arguments $\mathbf{k}$, $\mathbf{k}'$; the second two exhibit anti-symmetry. Decoupling the symmetric part,

$$c_xc'_x + c_yc'_y = \frac{1}{2}(c_x+c_y)(c'_x+c'_y) + \frac{1}{2}(c_x-c_y)(c'_x-c'_y)$$

which finally gives:

$$\begin{aligned}\cos\left(\delta k_x\right) + \cos\left(\delta k_y\right) = {}& \frac{1}{2}(c_x+c_y)(c'_x+c'_y) && (s^*\text{-wave})\\ &+ s_xs'_x && (p_x\text{-wave})\\ &+ s_ys'_y && (p_y\text{-wave})\\ &+ \frac{1}{2}(c_x-c_y)(c'_x-c'_y) && (d_{x^2-y^2}\text{-wave})\end{aligned}$$

In other words, the two-body potential decomposes as

$$\begin{aligned}V_{\mathbf{k}\mathbf{k}'} &= \sum_\gamma V^{(\gamma)}\varphi^{(\gamma)}_{\mathbf{k}}\varphi^{(\gamma)*}_{\mathbf{k}'} \qquad\qquad \text{where} \quad \gamma = s^*, p_x, p_y, d_{x^2-y^2}\\ &= \frac{V}{L_xL_y}\sum_\gamma \varphi^{(\gamma)}_{\mathbf{k}}\varphi^{(\gamma)*}_{\mathbf{k}'}\end{aligned}$$

being $\varphi^{(\gamma)}_{\mathbf{k}}$ the reciprocal-space expressions for the form factors of Tab. 3.2, listed explicitly in Tab. 3.3, and $V^{(\gamma)}_{\mathbf{k}\mathbf{k}'}$ the symmetry-resolved components of the non-local attraction. Then the

Structure	Structure factor	Graph
s-wave	$\varphi_{\mathbf{k}}^{(s)} = 1$	Fig. 3.1a
Extended s-wave	$\varphi_{\mathbf{k}}^{(s^*)} = \cos k_x + \cos k_y$	Fig. 3.1b
p_x-wave	$\varphi_{\mathbf{k}}^{(p_x)} = i\sqrt{2}\sin k_x$	Fig. 3.1c
p_y-wave	$\varphi_{\mathbf{k}}^{(p_y)} = i\sqrt{2}\sin k_y$	Fig. 3.1d
$d_{x^2-y^2}$-wave	$\varphi_{\mathbf{k}}^{(d)} = \cos k_x - \cos k_y$	Fig. 3.1e

Table 3.3 | Structure factors derived from the correlation structures of Tab. **??**. The functions hereby defined are orthonormal, and define the various components of the non-local topological effective potential.

two-body potential has been decomposed in its planar symmetry components, each of which will naturally couple only to identically structured parameters in the full hamiltonian.

Define now the non-local gap function

$$\mathcal{V}_{\mathbf{k}} \equiv \sum_{\mathbf{k}'} V_{\mathbf{k}\mathbf{k}'} \langle \hat{\phi}_{\mathbf{k}'}^\dagger \rangle \tag{3.6}$$

one gets immediately

$$\hat{H}_V \simeq -\sum_{\mathbf{k}} \left[\mathcal{V}_{\mathbf{k}} \hat{\phi}_{\mathbf{k}} + \mathcal{V}_{\mathbf{k}}^* \hat{\phi}_{\mathbf{k}}^\dagger \right] \tag{3.7}$$

To assume symmetry is broken in a specific symmetry channel γ means precisely to assume $g_{ij} \propto \varphi_{ij}^{(\gamma)}$, which in turn implies $\langle \hat{\phi}_{\mathbf{k}} \rangle \propto \varphi_{\mathbf{k}}^{(\gamma)}$. Of course, in Eq. (3.6) only the γ component of the potential survives, implying the gap function acquires the same symmetry,

$$\begin{aligned} \mathcal{V}_{\mathbf{k}} &\propto \sum_{\mathbf{k}'} \frac{V}{L_x L_y} \varphi_{\mathbf{k}}^{(\gamma)} \varphi_{\mathbf{k}'}^{(\gamma)*} \varphi_{\mathbf{k}'}^{(\gamma)} \\ &\propto \varphi_{\mathbf{k}}^{(\gamma)} \end{aligned}$$

where I used orthonormality of the $\varphi_{\mathbf{k}}^{(\gamma)}$ functions.

3.3.3 Local interaction and gap function

A very similar argument can be carried out for the local U term. Without delving in too many details, the local gap $\mathcal{U}_{\mathbf{k}}$ is given by

$$\mathcal{U}_{\mathbf{k}} \equiv \frac{U}{2L_x L_y} \sum_{\mathbf{k}} \langle \hat{\phi}_{\mathbf{k}} \rangle \tag{3.8}$$

evidently independent of $\mathbf{k}$, correctly. Identical considerations as in the above section hold for the local gap. The local part of the hamiltonian then gets

$$\hat{H}_U \simeq \sum_{\mathbf{k}} \left[\mathcal{U}_{\mathbf{k}} \hat{\phi}_{\mathbf{k}} + \mathcal{U}_{\mathbf{k}}^* \hat{\phi}_{\mathbf{k}}^\dagger \right] \tag{3.9}$$

and the full gap function is simply

$$\Delta_{\mathbf{k}} \equiv \mathcal{V}_{\mathbf{k}} - \mathcal{U}_{\mathbf{k}} \tag{3.10}$$

Notice here that the only possible topology here is s-wave; define trivially the s-wave component of the total two-body interaction,

$$V^{(s)} = -\frac{U}{2L_x L_y}$$

Then the full effective interaction is collected in

$$\begin{aligned}\hat{H}_U + \hat{H}_V &\simeq -\sum_{\gamma}\sum_{\mathbf{k},\mathbf{k}'} V^{(\gamma)}\varphi^{(\gamma)}_{\mathbf{k}}\varphi^{(\gamma)*}_{\mathbf{k}'}\left[\langle\hat{\phi}^{\dagger}_{\mathbf{k}}\rangle\hat{\phi}_{\mathbf{k}'} + \langle\hat{\phi}_{\mathbf{k}}\rangle\hat{\phi}^{\dagger}_{\mathbf{k}'}\right] \\ &= -\sum_{\mathbf{k}}\left[\Delta_{\mathbf{k}}\hat{\phi}_{\mathbf{k}} + \Delta^{*}_{\mathbf{k}}\hat{\phi}^{\dagger}_{\mathbf{k}}\right]\end{aligned}$$

The full self-consistency equation is given by

$$\Delta_{\mathbf{k}} \equiv \sum_{\mathbf{k}'}\left[V^{(s)} + V_{\mathbf{k}\mathbf{k}'}\right]\langle\hat{\phi}^{\dagger}_{\mathbf{k}'}\rangle \tag{3.11}$$

The gap function decomposes in symmetry channels as well,

$$\Delta_{\mathbf{k}} = \sum_{\gamma}\Delta^{(\gamma)}\varphi^{(\gamma)}_{\mathbf{k}}$$

If SC arises in a specific symmetry channel, $\Delta_{\mathbf{k}}$ will show the same symmetry. It follows, due to orthonormality and using Eq. (3.11),

$$\begin{aligned}\Delta^{(\gamma)} &= \frac{1}{L_x L_y}\sum_{\mathbf{k}}\varphi^{(\gamma)*}_{\mathbf{k}}\Delta_{\mathbf{k}} \\ &= \frac{1}{L_x L_y}\sum_{\mathbf{k}}\varphi^{(\gamma)*}_{\mathbf{k}}\sum_{\mathbf{k}'}\left[V^{(s)} + V_{\mathbf{k}\mathbf{k}'}\right]\langle\hat{\phi}^{\dagger}_{\mathbf{k}'}\rangle \\ &= \frac{1}{L_x L_y}\sum_{\mathbf{k}}\varphi^{(\gamma)*}_{\mathbf{k}}\sum_{\mathbf{k}'\gamma'}V^{(\gamma')}\varphi^{(\gamma')}_{\mathbf{k}}\varphi^{(\gamma')*}_{\mathbf{k}'}\langle\hat{\phi}^{\dagger}_{\mathbf{k}'}\rangle \\ &= V^{(\gamma)}\sum_{\mathbf{k}}\varphi^{(\gamma)*}_{\mathbf{k}}\langle\hat{\phi}^{\dagger}_{\mathbf{k}}\rangle\end{aligned} \tag{3.12}$$

This result provides a set of self-consistency equations for each symmetry channel, listed in Tab. 3.4. Notice that to reconstruct self-consistently the full s-wave phase transition, the actual gap function is given by

$$\Delta^{(s)} + \Delta^{(s^*)}(c_x + c_y)$$

The s-wave transition is the only one equipped of both the local and the non-local parts. Within this structure, we are finally able to move to Nambu formalism.

3.3.4 Nambu formalism and Bogoliubov transform

Define the Nambu spinor[1] as in BCS

$$\hat{\Psi}_{\mathbf{k}} \equiv \begin{bmatrix}\hat{c}_{\mathbf{k}\uparrow} \\ \hat{c}^{\dagger}_{-\mathbf{k}\downarrow}\end{bmatrix}$$

Evidently,

$$\phi_{\mathbf{k}} = \hat{\Psi}^{\dagger}_{\mathbf{k}}\begin{bmatrix}0 & 1 \\ 0 & 0\end{bmatrix}\hat{\Psi}_{\mathbf{k}} \qquad \phi^{\dagger}_{\mathbf{k}} = \hat{\Psi}^{\dagger}_{\mathbf{k}}\begin{bmatrix}0 & 0 \\ 1 & 0\end{bmatrix}\hat{\Psi}_{\mathbf{k}} \tag{3.13}$$

The full hamiltonian is then given by:

$$\hat{H} = \sum_{\mathbf{k}}\hat{\Psi}_{\mathbf{k}}h_{\mathbf{k}}\hat{\Psi}_{\mathbf{k}} \qquad h_{\mathbf{k}} \equiv \begin{bmatrix}\epsilon_{\mathbf{k}} & -\Delta^{*}_{\mathbf{k}} \\ -\Delta_{\mathbf{k}} & -\epsilon_{\mathbf{k}}\end{bmatrix} \tag{3.14}$$

Let τ^{α} for $\alpha = x, y, z$ be the Pauli matrices. Define:

$$\hat{s}^{\alpha}_{\mathbf{k}} \equiv \hat{\Psi}^{\dagger}_{\mathbf{k}}\tau^{\alpha}\hat{\Psi}_{\mathbf{k}} \quad \text{for} \quad \alpha = x, y, z$$

[1] Notice that the spinor is here differently defined with respect to App. **??**, where because of the HF prevalence in mean-field decoupling the spinor components were homogeneously fermions creations or destructions.

Structure	Self-consistency equation	Graph
s-wave	$\Delta^{(s)} = -\frac{U}{2L_xL_y}\sum_{\mathbf{k}}\langle\hat{\phi}^\dagger_{\mathbf{k}}\rangle$	Fig. 3.1a
Extended s-wave	$\Delta^{(s^*)} = \frac{V}{L_xL_y}\sum_{\mathbf{k}}(c_x+c_y)\langle\hat{\phi}^\dagger_{\mathbf{k}}\rangle$	Fig. 3.1b
p_x-wave	$\Delta^{(p_x)} = -i\sqrt{2}\frac{V}{L_xL_y}\sum_{\mathbf{k}} s_x\langle\hat{\phi}^\dagger_{\mathbf{k}}\rangle$	Fig. 3.1c
p_y-wave	$\Delta^{(p_y)} = -i\sqrt{2}\frac{V}{L_xL_y}\sum_{\mathbf{k}} s_y\langle\hat{\phi}^\dagger_{\mathbf{k}}\rangle$	Fig. 3.1d
$d_{x^2-y^2}$-wave	$\Delta^{(d)} = \frac{V}{L_xL_y}\sum_{\mathbf{k}}(c_x-c_y)\langle\hat{\phi}^\dagger_{\mathbf{k}}\rangle$	Fig. 3.1e

Table 3.4 | Symmetry resolved self-consistency equations for the MFT parameters $\Delta^{(\gamma)}$, based on Eq. (3.11) and (3.12). By computing $\langle\hat{\phi}^\dagger_{\mathbf{k}}\rangle$, it is possible to reconstruct the various components of the gap function.

As can be shown easily, these operators realize spin-1/2 algebra. $\hat{H}$ represents an ensemble of L_xL_y independent spins subject to pseudo-magnetic fields. Note that, differently form App. **??** where the chemical potential is inserted later (because in Nambu formalism it accounts for a diagonal term) here the chemical potential is part of the z component of the pseudo-magnetic field, since

$$\begin{aligned}\hat{n}_{\mathbf{k}\uparrow}+\hat{n}_{-\mathbf{k}\downarrow} &= \hat{c}^\dagger_{\mathbf{k}\uparrow}\hat{c}_{\mathbf{k}\uparrow}+\hat{c}^\dagger_{-\mathbf{k}\downarrow}\hat{c}_{-\mathbf{k}\downarrow}\\ &= \hat{c}^\dagger_{\mathbf{k}\uparrow}\hat{c}_{\mathbf{k}\uparrow}-\hat{c}_{-\mathbf{k}\downarrow}\hat{c}^\dagger_{-\mathbf{k}\downarrow}+\mathbb{I}\\ &= \hat{\Psi}^\dagger_{\mathbf{k}}\tau^z\hat{\Psi}_{\mathbf{k}}+\mathbb{I}\end{aligned} \tag{3.15}$$

and then it follows

$$\begin{aligned}-\mu\hat{N} &= -\mu\sum_{\mathbf{k}\in\mathrm{BZ}}[\hat{n}_{\mathbf{k}\uparrow}+\hat{n}_{-\mathbf{k}\downarrow}]\\ &= -\mu\sum_{\mathbf{k}\in\mathrm{BZ}}\hat{\Psi}^\dagger_{\mathbf{k}}\tau^z\hat{\Psi}_{\mathbf{k}}-\mu L_xL_y\end{aligned}$$

Then, adding a term $-\mu\hat{N}$ to $\hat{H}$, apart from an irrelevant total energy increase, changes the pseudo-field whose explicit form becomes

$$\mathbf{b}_{\mathbf{k}} \equiv \begin{bmatrix}-\mathrm{Re}\{\Delta_{\mathbf{k}}\}\\ -\mathrm{Im}\{\Delta_{\mathbf{k}}\}\\ \epsilon_{\mathbf{k}}-\mu\end{bmatrix} \tag{3.16}$$

This hamiltonian behaves as an ensemble of spins in local magnetic fields precisely as in Eq. (**??**),

$$\hat{H}-\mu\hat{N} = \sum_{\mathbf{k}\in\mathrm{BZ}}\mathbf{b}_{\mathbf{k}}\cdot\hat{\mathbf{s}}_{\mathbf{k}} \quad \text{where} \quad \hat{\mathbf{s}}_{\mathbf{k}\sigma} = \begin{bmatrix}\hat{s}^x_{\mathbf{k}}\\ \hat{s}^y_{\mathbf{k}}\\ \hat{s}^z_{\mathbf{k}}\end{bmatrix} \tag{3.17}$$

Proceed as in App. **??** and diagonalize via a rotation,

$$d_{\mathbf{k}} \equiv \begin{bmatrix}-E_{\mathbf{k}} & \\ & E_{\mathbf{k}}\end{bmatrix} \quad \text{being} \quad E_{\mathbf{k}} \equiv \sqrt{\xi^2_{\mathbf{k}}+|\Delta_{\mathbf{k}}|^2}$$

and $\xi_{\mathbf{k}} \equiv \epsilon_{\mathbf{k}}-\mu$. Given the pseudoangles

$$\tan(2\theta_{\mathbf{k}}) \equiv \frac{|\Delta_{\mathbf{k}}|}{\epsilon_{\mathbf{k}}} \qquad \tan(2\zeta_{\mathbf{k}}) \equiv \frac{\mathrm{Im}\{\Delta_{\mathbf{k}}\}}{\mathrm{Re}\{\Delta_{\mathbf{k}}\}}$$

the general diagonalizer will be an orthogonal rotation matrix

$$\begin{aligned} W_{\mathbf{k}} &= e^{i\left(\theta_{\mathbf{k}}-\frac{\pi}{2}\right)\tau^y} e^{i\zeta_{\mathbf{k}}\tau^z} \\ &= \begin{bmatrix} -\sin\theta_{\mathbf{k}} & -\cos\theta_{\mathbf{k}} \\ \cos\theta_{\mathbf{k}} & -\sin\theta_{\mathbf{k}} \end{bmatrix} \begin{bmatrix} e^{i\zeta_{\mathbf{k}}} & \\ & e^{-i\zeta_{\mathbf{k}}} \end{bmatrix} \\ &= \begin{bmatrix} -\sin\theta_{\mathbf{k}} e^{i\zeta_{\mathbf{k}}} & -\cos\theta_{\mathbf{k}} e^{-i\zeta_{\mathbf{k}}} \\ \cos\theta_{\mathbf{k}} e^{i\zeta_{\mathbf{k}}} & -\sin\theta_{\mathbf{k}} e^{-i\zeta_{\mathbf{k}}} \end{bmatrix} \end{aligned} \tag{3.18}$$

given by a rotation of angle $\zeta_{\mathbf{k}}$ around the z axis, to align the x axis with the field projection onto the xy plane, followed by a rotation around the y axis to anti-align with the pseudo-field. The MFT-BCS solution is given by a degenerate Fermi gas at ground state, whose quasi-particles occupy two bands $\pm E_{\mathbf{k}}$ and their fermionic operators are given by

$$\hat{\gamma}_{\mathbf{k}}^{(-)} \equiv \left[W_{\mathbf{k}}\hat{\Psi}_{\mathbf{k}}\right]_1 \qquad \hat{\gamma}_{\mathbf{k}}^{(+)} \equiv \left[W_{\mathbf{k}}\hat{\Psi}_{\mathbf{k}}\right]_2$$

The diagonalization operators are given by

$$\hat{\Gamma}_{\mathbf{k}} \equiv W_{\mathbf{k}}\hat{\Psi}_{\mathbf{k}} \quad \text{where} \quad \hat{\Gamma}_{\mathbf{k}} = \begin{bmatrix} \hat{\gamma}_{\mathbf{k}}^{(-)} \\ \hat{\gamma}_{\mathbf{k}}^{(+)} \end{bmatrix}$$

then, using Eq. (**??**),

$$\left\langle [\hat{\Psi}_{\mathbf{k}}^\dagger]_i [\hat{\Psi}_{\mathbf{k}}]_j \right\rangle = [W_{\mathbf{k}}]_{1i}[W_{\mathbf{k}}^\dagger]_{j1} f\left(-E_{\mathbf{k}};\beta,0\right) + [W_{\mathbf{k}}]_{2i}[W_{\mathbf{k}}^\dagger]_{j2} f\left(E_{\mathbf{k}};\beta,0\right)$$

where in the Fermi-Dirac function chemical potential was set to zero, because it already was included in the diagonalized hamiltonian. Recalling Eq. (**??**), it follows

$$\langle \phi_{\mathbf{k}}^\dagger \rangle = [W_{\mathbf{k}}]_{11}[W_{\mathbf{k}}^\dagger]_{21} f\left(-E_{\mathbf{k}};\beta,0\right) + [W_{\mathbf{k}}]_{21}[W_{\mathbf{k}}^\dagger]_{22} f\left(E_{\mathbf{k}};\beta,0\right) \tag{3.19}$$

$$= \frac{1}{2}\sin\left(2\theta_{\mathbf{k}}\right) e^{i2\zeta_{\mathbf{k}}} \tanh\left(\frac{\beta E_{\mathbf{k}}}{2}\right) \tag{3.20}$$

The last passage has been obtained by computing the matrix element from the explicit form of $W_{\mathbf{k}}$ of Eq. (3.18) and by the simple relation

$$\begin{aligned} \frac{1}{e^{-x}+1} - \frac{1}{e^{x}+1} &= \frac{e^x - 1}{e^x + 1} \\ &= \tanh\left(\frac{x}{2}\right) \end{aligned}$$

Eqns. (3.19), (3.20) give us both the algorithmic formula (first row) and its theoretical counterpart (second row) to compute the order parameters in the HF approach at each point in k-space (k_x, k_y). We can finally derive the BCS self-consistency equation

$$\Delta_{\mathbf{k}} \equiv \frac{1}{2}\sum_{\mathbf{k}'}\left[V^{(s)} + V_{\mathbf{k}\mathbf{k}'}\right] \frac{|\Delta_{\mathbf{k}}|}{\sqrt{\xi_{\mathbf{k}}^2 + |\Delta_{\mathbf{k}}|^2}} e^{i\,\mathrm{Im}\{\Delta_{\mathbf{k}}\}/\,\mathrm{Re}\{\Delta_{\mathbf{k}}\}} \tanh\left(\frac{\beta}{2}\sqrt{\xi_{\mathbf{k}}^2 + |\Delta_{\mathbf{k}}|^2}\right) \tag{3.21}$$

The whole point of the HF algorithm is to find an iterative solution for each symmetry channel, using the self-consistency equation projection of Tab. 3.4.

Notice that the z component of the spin operators is related to density: using Eq. (**??**),

$$\langle \hat{\Psi}_{\mathbf{k}}^\dagger \tau^z \hat{\Psi}_{\mathbf{k}} \rangle = \left\langle [\hat{\Psi}_{\mathbf{k}}^\dagger]_1 [\hat{\Psi}_{\mathbf{k}}]_1 \right\rangle - \left\langle [\hat{\Psi}_{\mathbf{k}}^\dagger]_2 [\hat{\Psi}_{\mathbf{k}}]_2 \right\rangle$$

I proceed in as done previously, and from Eq. (3.15),

$$\begin{aligned} \langle \hat{n}_{\mathbf{k}\uparrow} \rangle + \langle \hat{n}_{-\mathbf{k}\downarrow} \rangle &= 1 + \langle \hat{\Psi}_{\mathbf{k}}^\dagger \tau^z \hat{\Psi}_{\mathbf{k}} \rangle \\ &= 1 + \left(|[W_{\mathbf{k}}]_{11}|^2 - |[W_{\mathbf{k}}]_{12}|^2 \right) f\left(-E_{\mathbf{k}};\beta,0\right) \\ &\quad + \left(|[W_{\mathbf{k}}]_{21}|^2 - |[W_{\mathbf{k}}]_{22}|^2 \right) f\left(E_{\mathbf{k}};\beta,0\right) \qquad (3.22) \\ &= 1 - \cos\left(2\theta_{\mathbf{k}}\right) \tanh\left(\frac{\beta E_{\mathbf{k}}}{2}\right) \qquad (3.23) \end{aligned}$$

The expectation value for the density is needed in order to extract the optimal chemical potential μ for the target density we aim to simulate at the given parametrization. This is numerically obtained by using Eq. (3.22) directly on the diagonalization matrix of $h_{\mathbf{k}}$.

3.3.5 A short comment on self-consistency

The Bogoliubov fermions in spinor representation satisfy obviously $\hat{\Psi}_{\mathbf{k}} = W_{\mathbf{k}}^{\dagger}\hat{\Gamma}_{\mathbf{k}}$. Consider e.g.

$$\langle \hat{c}^{\dagger}_{\mathbf{k}\sigma}\hat{c}^{\dagger}_{-\mathbf{k}\sigma}\rangle$$

which is a spin-symmetric anomalous Cooper pair. For simplicity, take $\sigma =\uparrow$. Expand:

$$\begin{aligned}\langle \hat{c}^{\dagger}_{\mathbf{k}\uparrow}\hat{c}^{\dagger}_{-\mathbf{k}\uparrow}\rangle &= \left\langle [\hat{\Psi}^{\dagger}_{\mathbf{k}}]_1[\hat{\Psi}^{\dagger}{}_{-\mathbf{k}}]_1 \right\rangle \\ &= \left\langle [W_{\mathbf{k}}\hat{\Gamma}^{\dagger}_{\mathbf{k}}]_1[W_{-\mathbf{k}}\hat{\Gamma}^{\dagger}{}_{-\mathbf{k}}]_1 \right\rangle\end{aligned}$$

This expectation value is taken over the ground-state, the latter being the vacuum of Γ fermions. Evidently the above expectation cannot assume non-zero values. Obviously the same holds for $\sigma =\downarrow$, and this argument explains why the Ferromagnetic terms of the hamiltonian decomposition do not contribute to Cooper instability. An identical argument, with the exchange

$$(\sigma,\sigma)\to(\uparrow,\downarrow) \quad \text{and} \quad (\mathbf{k},-\mathbf{k})\to(\mathbf{K}+\mathbf{k},\mathbf{K}-\mathbf{k}) \quad \text{with} \quad \mathbf{K}\neq\mathbf{0}$$

justifies why in Sec. 3.3.4 the only relevant contribution was given by $\mathbf{K}=\mathbf{0}$. In the next sections, the results of the self-consistent HF algorithm are exposed.

3.4 Results of the HF algorihtm

[To be continued...]

Bibliography

[1] Zhangkai Cao et al. *p-wave superconductivity induced by nearest-neighbor attraction in the square-lattice extended Hubbard model*. en. arXiv:2408.01113 [cond-mat]. Jan. 2025. DOI: 10.48550/arXiv.2408.01113. URL: http://arxiv.org/abs/2408.01113 (visited on 03/15/2025).

[2] Piers Coleman. *Introduction to Many-Body Physics*. Cambridge University Press, 2015.

[3] Michele Fabrizio. *A Course in Quantum Many-Body Theory*. Springer, 2022.

[4] Gabriele Giuliani and Giovanni Vignale. *Quantum Theory of the Electron Liquid*. Cambridge University Press, 2005.

[5] Giuseppe Grosso and Giuseppe Pastori Parravicini. *Solid State Physics*. Second Edition. Academic Press, 2014.

[6] J. E. Hirsch. "Two-dimensional Hubbard model: Numerical simulation study". In: *Phys. Rev. B* 31 (7 Apr. 1985), pp. 4403–4419. DOI: 10.1103/PhysRevB.31.4403. URL: https://link.aps.org/doi/10.1103/PhysRevB.31.4403.

[7] Robin Scholle et al. "Comprehensive mean-field analysis of magnetic and charge orders in the two-dimensional Hubbard model". In: *Phys. Rev. B* 108 (3 July 2023), p. 035139. DOI: 10.1103/PhysRevB.108.035139. URL: https://link.aps.org/doi/10.1103/PhysRevB.108.035139.